

Microbial Community Biofabrics in a Geothermal Mine Adit^{∇†}

John R. Spear,¹ Hazel A. Barton,² Charles E. Robertson,³
Christopher A. Francis,⁴ and Norman R. Pace^{3*}

Division of Environmental Science and Engineering, Colorado School of Mines, Golden, Colorado 80401¹; Department of Biological Sciences, Northern Kentucky University, SC 204D Nunn Drive, Highland Heights, Kentucky²; Department of Molecular, Cellular, and Developmental Biology, 347 UCB, University of Colorado at Boulder, Boulder, Colorado 80309³; and Department of Geological and Environmental Sciences, Stanford University, Stanford, California 94305⁴

Received 19 February 2007/Accepted 30 July 2007

Speleothems such as stalactites and stalagmites are usually considered to be mineralogical in composition and origin; however, microorganisms have been implicated in the development of some speleothems. We have identified and characterized the biological and mineralogical composition of mat-like biofabrics in two novel kinds of speleothems from a 50°C geothermal mine adit near Glenwood Springs, CO. One type of structure consists of 2- to 3-cm-long, 3- to 4-mm-wide, leather-like, hollow, soda straw stalactites. Light and electron microscopy indicated that the stalactites are composed of a mineralized biofabric with several cell morphotypes in a laminated form, with gypsum and sulfur as the dominant mineral components. A small-subunit rRNA gene phylogenetic community analysis along the stalactite length yielded a diverse gradient of organisms, with a relatively simple suite of main constituents: *Thermus* spp., crenarchaeotes, *Chloroflexi*, and *Gammaproteobacteria*. PCR analysis also detected putative crenarchaeal ammonia monooxygenase subunit A (*amoA*) genes in this community, the majority related to sequences from other geothermal systems. The second type of speleothem, dumpling-like rafts floating on a 50°C pool on the floor of the adit, showed a mat-like fabric of evidently living organisms on the outside of the dumpling, with a multimineral, amorphous, gypsum-based internal composition. These two novel types of biofabrics are examples of the complex roles that microbes can play in mineralization, weathering, and deposition processes in karst environments.

Caves provide an entrance into the subsurface world and consequently are natural laboratories for the study of the mineralogy and biology of the subsurface. Cave passages often are decorated with secondary features such as stalactites and stalagmites, which, as with ice cores and tree rings, can serve as records of past biological and paleoclimate activity (3–5, 36). Most secondary deposits are considered mineralogical in formation, but some secondary mineral deposits have a microbiological component to their formation (7, 8, 13, 33, 34, 38). Microbes potentially influence mineral deposition in many ways, for instance by bioprecipitation, biomineralization, and alteration of the rock substrate (11, 12, 22, 44).

Caves are sometimes associated with geothermally warmed subsurface waters, which can accelerate cave formation by increased calcium carbonate dissolution (26). Hot springs within cave passages fill the cave with geothermally warmed gases and steam to produce “vapor caves.” The vapor/aerosol can be rich not only in water but also in gases such as H₂ and H₂S, which in combination with mineral surfaces are potential energy sources to promote lithotrophic microbial life (9, 19, 20). Such microbial life can be evidenced by “slime” on cave walls, discoloration of cave limestone matrix, powderization of the cave matrix, and fabric-like speleothem formations (6). Microbial

growth on cave walls is evident in both sulfidic and nonsulfidic caves (6, 15, 36, 39–42).

We report here an analysis of novel biofabrics, complex associations of microbes in a weave of mineralization, associated with two kinds of speleothems from a geothermally heated 50°C mine adit near Glenwood Springs, on Colorado’s western slope. The walls and ceilings of the adit have patches of a slimy microbial mat, from which descend short (2- to 3-cm) leather-like stalactites. Floating in pools on the floor of the adit are dumpling-like “cave rafts” of various sizes and shapes, which can be as thick as 10 cm. Both of these features presumably formed from mineralogical precipitation of calcite and/or gypsum, but a biological role in the process seemed possible, and preliminary microscopy indicated the occurrence of conspicuous microbiological activity in both structures. Little is known about the kinds of organisms that are associated with the mineralization processes within caves. Consequently, we sought to explore the biological component of these novel speleothems.

MATERIALS AND METHODS

Sample collection. The mine adit lies approximately 3 m below the surface; it is 50 m in length and is filled with 49.6°C water in spring-fed pools. The source of this hot water is the Leadville aquifer, which is responsible for the water chemistry observed: pH 6.4, 1.65 mg/liter dissolved hydrogen sulfide, and 2.5 mg/liter dissolved oxygen (44% saturation at this temperature and atmospheric pressure) (8). Due to reduced oxygen, at 7.5% atmospheric oxygen, limited visibility from the high vapor/fog content, an air temperature of 49.6°C, and difficulties associated with walking/standing in hot water, sampling trips were short in duration. In August 2004, sampling trips were made to retrieve two “stalactites,” a sample of the ceiling microbial mat, and a sample of a floating “dumpling” for phylogenetic and microscopic analysis. Samples for phylogenetic analysis were transported back to the lab at 4°C (<4 h) and stored at –80°C.

* Corresponding author. Mailing address: Department MCD-Biology, 347 UCB, University of Colorado at Boulder, Boulder, CO 80309. Phone: (303) 735-1808. Fax: (303) 492-7744. E-mail: nrpace@colorado.edu.

† Supplemental material for this article may be found at <http://aem.asm.org/>.

∇ Published ahead of print on 10 August 2007.

Samples for microscopic analysis were placed in 4% paraformaldehyde-phosphate-buffered saline at room temperature for 2 h, washed in 1× phosphate-buffered saline, and stored in 50% ethanol at 4°C.

Molecular phylogenetic analyses. Total community DNA was obtained and prepared from ~1 g of the frozen samples as previously described (18, 45), with an average yield of 600 ng/μl in 30 μl of extract. Initial PCR amplifications were performed with the universal small-subunit rRNA degenerate primers 515F (5'-GTGCCAGCMGCCGCGGTAA3') and 1391R (5'-GACGGGCGGTGWGTCA3') (29). PCRs were carried out in an Eppendorf gradient thermocycler at 94°C for 2 min followed by 29 cycles at 94°C for 30 s, 55.5°C for 1 min, and 72°C for 1.5 min followed by a 72°C step for 12 min. Each 25-μl reaction mixture contained 30 mM Tris (pH 8.4), 50 mM KCl, 1.5 mM MgCl₂, 0.05% bovine serum albumin (Sigma), 1 M betaine, 0.2 mM of each deoxynucleotide triphosphate, 50 ng of each oligonucleotide primer, 0.5 units of *Taq* polymerase, and approximately 600 ng of environmental DNA template. PCR products were gel purified using a QIAGEN gel extraction kit (QIAGEN, Inc., Valencia, CA) as per the kit instructions. Before cloning, 30 μl of gel-purified PCR product was incubated with 2 μl of deoxynucleotide triphosphates for 20 min at 72°C in 1× buffer, 1 U of *Taq* polymerase, and 1.5 mM MgCl₂. Reactions were cloned with the TOPO TA cloning kit for sequencing (Invitrogen, Carlsbad, CA), and unique restriction fragment length polymorphisms were sequenced with the DYEnamic ET Terminator cycle sequencing kit (Amersham Biosciences, Piscataway, NJ). Sequences were assembled with XplorSeq 1.0 (in-house software by Daniel Frank), and an initial identification was made via a BLAST search (www.ncbi.nlm.nih.gov/BLAST) (1). Clone libraries were compared in a phylogenetic context via the UniFrac method of Lozupone and Knight (31).

The software programs Mallard (2) and Bellerophon (25) were used to screen 16S rRNA gene sequence data for potential chimeras. Sequences flagged by either program as potentially chimeric were manually evaluated and rejected if suspect. Sequences that passed the screening process were aligned with the NAST aligner (17), and the aligned sequences were inserted, by parsimony insertion, into trees in the 16S rRNA database from greengenes.lbl.gov (16) that is compatible with the ARB (32) software package; ARB was used to construct all phylogenetic trees in this work. Sequence alignments used in phylogenetic analysis were minimized/masked using the Lane mask, with ~876-bp homologous nucleotide positions for phylogenetic analyses (29).

Functional gene analysis. For analysis of putative ammonia-oxidizing archaea (AOA), *amoA* gene fragments of ~635 bp were amplified using the PCR primers Arch-amoAF (5'-STAATGGTCTGGCTTAGACG-3') and Arch-amoAR (5'-GCGCCATCCATCTGTATGT-3') (21) by use of the following protocol: 95°C for 5 min and 30 cycles consisting of 94°C for 45 s, 53°C for 60 s, and 72°C for 1 min, followed by 72°C for 15 min. Triplicate PCRs were pooled, gel purified, cloned, and sequenced as described above. Archaeal *amoA* nucleotide sequences were assembled and edited using Sequencher 4.2 (GeneCodes, Ann Arbor, MI). Amino acid-based alignment of *amoA* DNA sequences was performed with the software transAlign (10). Maximum likelihood phylogenetic trees of the aligned *amoA* amino acid data set were constructed with RAxML (46). Bootstrap analysis was used to estimate the reliability of phylogenetic reconstructions (100 replicates). Branches with less than 70% support were deleted. To evaluate the richness within the archaeal *amoA* clone library, rarefaction analysis and Chao1 nonparametric richness estimations were performed using DOTUR (43). Operational taxonomic units (OTUs) were defined as sequence groups in which sequences differed by ≤5%.

SEM and energy-dispersive spectroscopy (EDS). Samples were washed in 70% ethanol and dehydrated in an ethanol series to 100%. Samples were dried in a critical point dryer with liquid CO₂. Half of the samples were examined under environmental scanning electron microscopy (SEM) conditions by use of an FEI Quanta 200 environmental SEM (ESEM) with a Princeton Gamma Tech Avalon microanalysis using secondary and backscatter electron detectors. The remaining samples were sputter coated with Au/Pd.

Nucleotide sequence accession numbers. 16S rRNA gene sequences have been deposited in GenBank under the accession numbers EF378701 to EF378943, while the *amoA* sequences have been deposited under accession numbers DQ672634 to DQ672715 and EF032877. The clone names for the 16S rRNA sequences reflect location as follows: GSST indicates Glenwood Springs, speleothem tip; GSSB indicates Glenwood Springs, speleothem base; GSCM indicates Glenwood Springs, ceiling mat; and GSCR indicates Glenwood Springs, cave raft.

RESULTS

Microscopy of stalactite biofabric. An ~2-cm leather-like soda straw stalactite, shown in Fig. 1A, was cut from the ceiling

biofilm, and three segments were taken for analysis: the ceiling mat/base; the base to middle ~1 cm, presumably the more mature component of the stalactite; and the ~1-cm “growing” tip. Phase-contrast microscopy and DAPI (4',6'-diamidino-2-phenylindole) fluorescence microscopy suggested that the wall of the stalactite was significantly biological in nature and complex in structure. Obvious variation included an ~10-fold-higher concentration of microbial cells along the outside of the stalactite than on the inside wall, adjacent to the lumen of the straw. To gain a more detailed view, we analyzed samples with an ESEM fitted with EDS (ESEM-EDS) for elemental analyses.

The microbial assemblage presumably responsible for the rubber-like structure of the speleothem is evident in the ESEM image mosaic shown in Fig. 1B to I. The central region of diffuse microbial cells (Fig. 1B to E) is surrounded by a sheath-like structural material. This sheath is comprised of what appear to be laminated, densely packed microbial filaments that are interwoven to form the biofabric (Fig. 1B to E). Embedded in the surfaces of these laminated layers are numerous crystals (Fig. 1D and E), indicated by ESEM-EDS to be comprised primarily of sulfur granules, consistent with the presence of these speleothems in a hydrogen sulfide-rich atmosphere. This biofabric-mineral matrix is consistent down the length of the soda straw and is similar in appearance to fabrics formed by some endolithic communities (50).

The structure of the inner wall of the stalactite is distinct from that of the outer surface, as shown in Fig. 1F to I. The inside is less densely packed but still forms a fabric comprised of two distinct morphotypes as follows: small, irregular spheres attached to filaments. Most of the fabric mass is associated with the wall, but some structures bridge hollows in the wall (Fig. 1G) along the entire length of the speleothem, possibly contributing to the structural stability of the formation.

Microscopy of adit wall. These stalactites descend from a biofilm on the limestone ceiling. Imaging of this biofilm by ESEM revealed finely structured biofabric-like layers (Fig. 1J to L) and, on the wall-proximal side, a red/brown corrosion residue possibly due to microbial activities. To gain insight into the mineralogy of the corrosion process, we examined the residue by ESEM-EDS, which detected iron, silica, and oxygen, suggesting the presence of iron oxides and silica-iron clays (see Fig. S1A to S1D in the supplemental material). The Leadville limestone in which the mine adit is found is nearly pure calcium carbonate (23), so we surmised that the iron oxides and clays represented insoluble material in the rock matrix that accumulates due to rock dissolution. To test this theory, we dissolved ~5 g of Leadville limestone (from the same location as the mine adit) in hydrochloric acid and determined that all nonsoluble particles had the same EDS profile as the red/brown corrosion residue on the wall adjacent to the biofilm. The results collectively suggest that biofilm actively dissolves the host rock.

We also used ESEM-EDS to inspect the host rock of the biofilm, a thin veneer of host limestone peeling away from the ceiling in locations where biofilm occurs. The results (see Fig. S1E to S1J in the supplemental material) suggested a significant structural change in the rock in direct contact with the biofilm, with a secondary mineralization on the surface of the host rock and the deposition of a sulfur-rich mineral. The

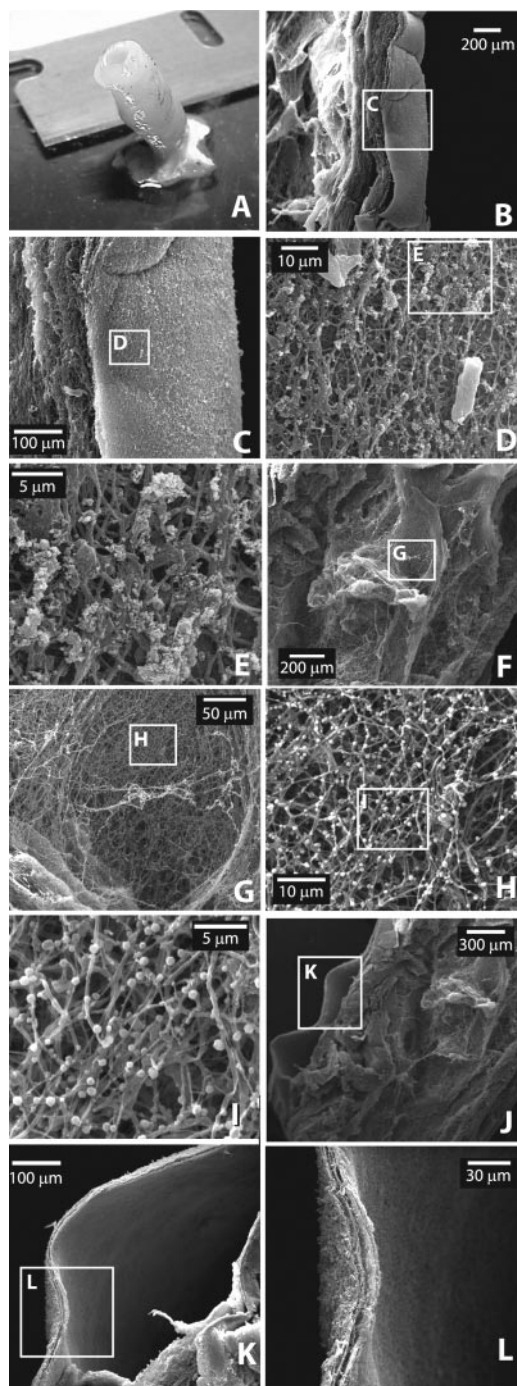


FIG. 1. (A) Photograph of a sectioned stalactite (tip removed) on a razor blade for scale (base, near blade). (B) ESEM image of the outer, leather-like wall of the “stalactite” with an outer “sheath” of structured material (center) that surrounds the hollow, central region of diffuse microbial cells (left). (C and D) Images demonstrate how the sheath material actually appears to be layers of densely packed microbiota of various morphologies, in which are embedded crystals of gypsum (CaSO_3 , as determined by ESEM-EDS). (E) A close-up view of the wall microbiota demonstrates intrabranched microbial cells, creating the observed laminated structure. This image also demonstrates the embedded crystals present packed in with the wall of the “stalactite.” (F) Central region of the inner structure of the stalactite of loosely packed microbial cells, with apparently cross-linking microbial structures. (G) Close-up image of cross-linking cells that span the hollow cylinder of the “stalactite.” (H) Close-up of the microbial cells that

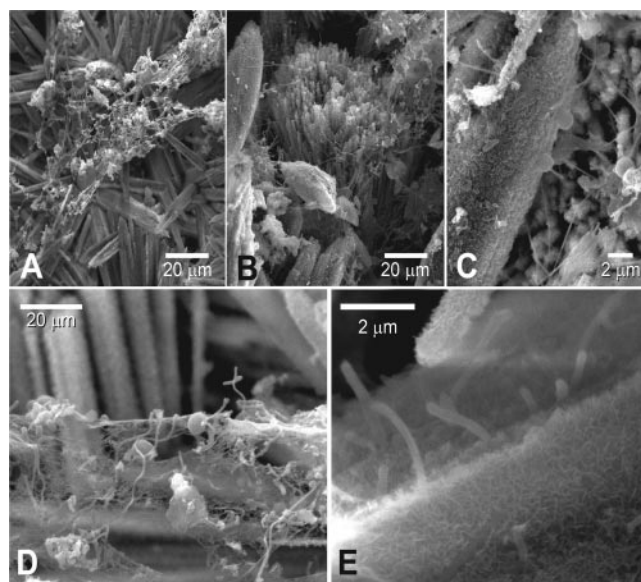


FIG. 2. ESEM images of the mineral consortia associated with the surface and inner portions of the floating “dumpling” structures. (A to C) Images demonstrate the presence of microbial consortia within the “dumpling” structures and clearly reveal the presence of gypsum crystals (confirmed by ESEM-EDS analysis) within this biogenic matrix. (D) A close-up image of microbial cells associated with the mineral matrix, demonstrating the production of polymeric substances. (E) An extreme close-up of the surface of the minerals associated with the “dumplings” indicates the presence of an EPS biofilm-like coating (the small projections from the biofilm average 50 nm in length).

high-sulfur material suggests the activity of sulfuric acid dissolution. The sulfur signature in the ESEM-EDS could be traced down into the rock, following miniscule cracks in the limestone host. Beyond the zones of apparent sulfur dissolution, the mineral was highly enriched in phosphate, which is not normally found in high concentrations in the Leadville limestone (23) and so could potentially serve as a biomarker.

Microscopy of “dumplings.” Floating on top of the 0.3-m-deep, 50°C, spring-fed pools along the length of the passage were 3- to 10-cm-thick mineral deposits we referred to as “dumplings” due to their unusual appearance. Unlike what is the case for typical mm-thick cave “rafts,” to our knowledge such thick dumplings have not been described previously. ESEM-EDS analysis of the dumpling speleothem (Fig. 2) showed that these structures are accumulations of amorphous gypsum surrounded by a morphologically complex community. EDS indicated a high carbon content in the outer fabric that surrounds the dumpling with a morphological appearance similar to that of extracellular polymeric substance (EPS) and a gypsum-like elemental signature from the inside. Different

comprise the structural form of the “stalactite.” (I) At the final resolution, the two morphologies of cells associated with the “stalactite” biofilm are readily apparent. (J) ESEM image of the adit wall biofilm and associated rock matrix. (K and L) Close-up of the biofilm shows packed microbial cells, with an apparent lamination of microbial structures.

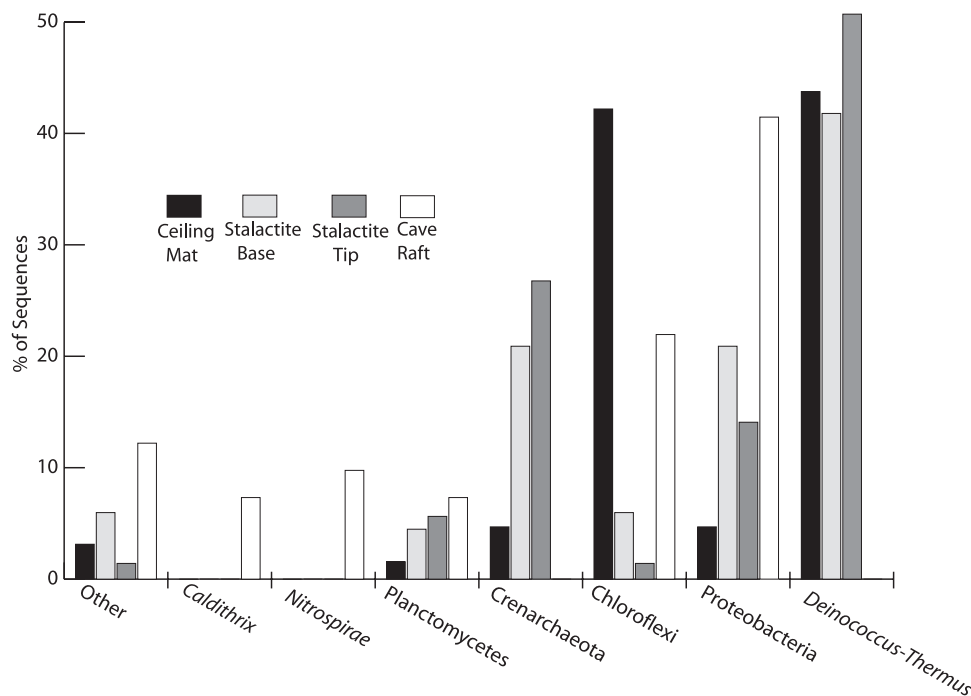


FIG. 3. Cumulative rRNA gene analyses with universal PCR primers (515F and 1391R) reflect the distribution of sequences by phylogenetic group, as identified by RAxML analysis and replacement in ARB.

crystal shapes are evident under the biofabric, with various cellular morphotypes evident (Fig. 2).

Phylogenetic composition of biofabrics. To identify the organisms associated with these biofabrics, we conducted phylogenetic analyses using rRNA gene sequences. Total DNA was extracted from three sections of the stalactite along its length (mat at base, base [~ 1 cm], and tip [~ 1 cm]) and from one bulk dumpling sample. PCR was carried out with the DNAs by use of the “universal” rRNA primer pair 515F/1391R, PCR products were cloned, and 96 randomly selected clones were sequenced per location. Although this number of clones likely would not sample all of the diversity of the communities, it provides an estimate of the phylogenetic composition of the main biomass.

Figure 3 shows the microbial community composition at the phylum (phylogenetic division) level for all four samples. The stalactite and dumpling communities differ considerably, with the stalactite community being less diverse. Generally, the same kinds of bacterial and archaeal phyla are located in all three regions of the stalactite, although the proportions differ markedly. No eucaryal sequences were detected among clones analyzed. In contrast to the stalactite community, the dumpling community is highly diverse (Fig. 3). The dumpling community contains many close relatives to known thermophilic heterotrophs, some related to organisms isolated from caves from many global locations, and no archaeal or eucaryal sequences were found.

The stalactite community exhibits a marked shift in phylogenetic makeup along its length from the cave ceiling mat to the tip of the stalactite (Fig. 3). Since our analysis probably undersamples the clone libraries, we tested if the observed results are statistically significant using the computer program

UniFrac (31). This analysis revealed marginally significant differences between the tip and ceiling mat (UniFrac P value, 0.018), while differences between base and ceiling mat ($P = 1.0$) and between base and tip ($P = 0.884$) were not significant (31).

Representatives of the *Thermus-Deinococcus* phylum are abundant in clone libraries from throughout the length of the stalactite. Phylogenetic analysis (Fig. 4A) shows that these sequences are of limited diversity, that they are the same group at a species-level proxy ($\geq 97\%$ rRNA sequence identity) throughout the stalactite, and that members correspond to the *Meiothermus* genus. Cultured examples of such organisms are moderately thermophilic heterotrophs. The other dominant (42%) group in the ceiling mat library, representatives of *Chloroflexi*, are almost absent from the tip community (2%). Phylogenetic analysis (Fig. 4B) shows that the stalactite sequences are mostly not specifically related to known sequences and are only distantly related to the few cultured representatives of the *Chloroflexi* phylum. *Gammaproteobacteria* rRNA genes are enriched severalfold from the mat (4%) to the tip (18%) and have closest relatives in sequences of organisms from soils and sediments. *Chloroflexi* sequences also are abundant in the dumpling library but were phylogenetically distinct from those in the stalactite libraries. As with soils and sediments, what metabolic capabilities these organisms are capable of, or engaged in, within these speleothem environments are unknown.

Another compositional difference between the stalactite libraries is the proportion of mesophilic *Crenarchaeota* 16S rRNA sequences from the ceiling mat (4%), the base (17%), and the tip (23%) of the stalactite (Fig. 3). Phylogenetic analysis (Fig. 4C) shows that these sequences are most closely related to clones previously recovered from service water ob-

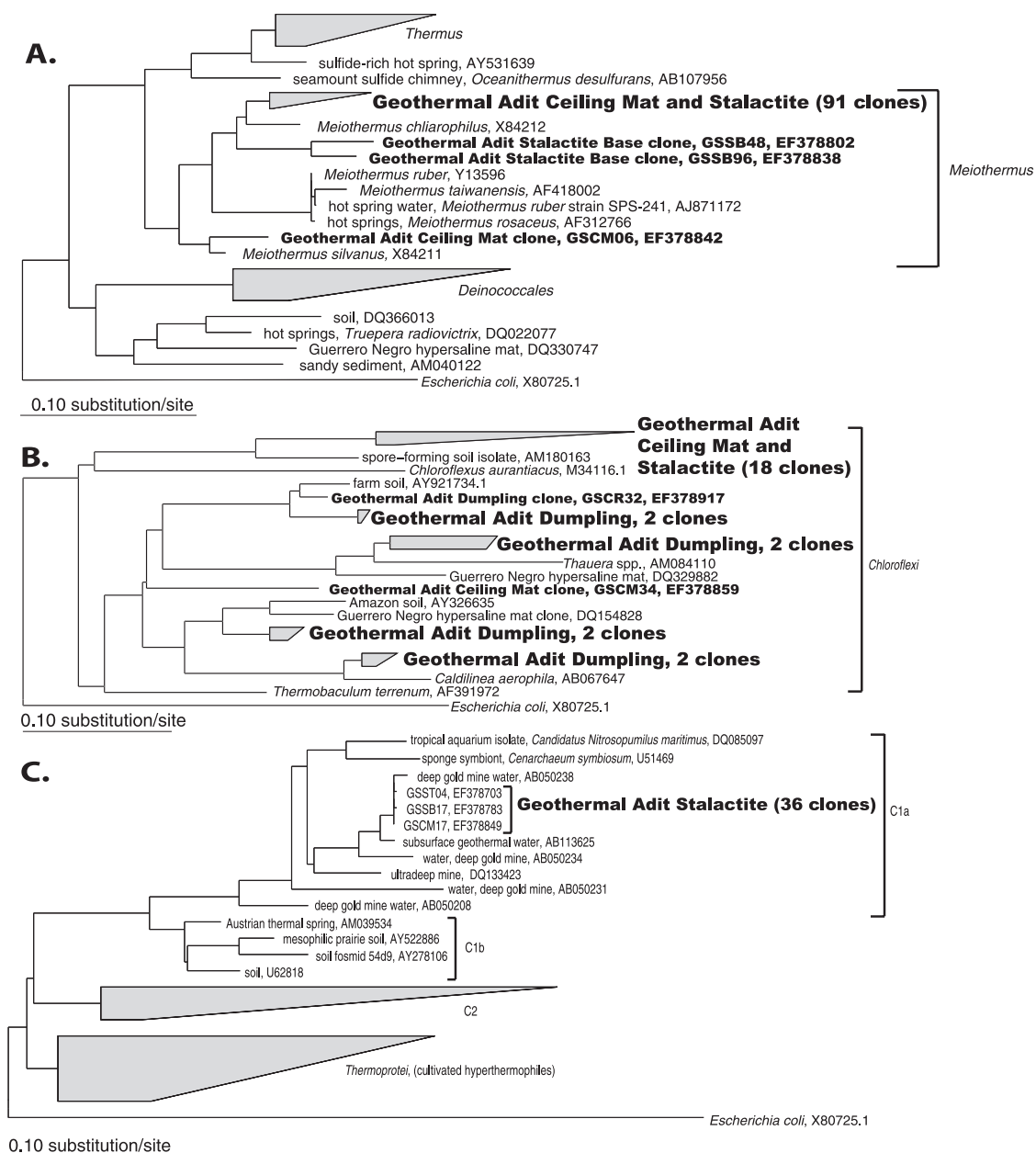


FIG. 4. Diagrammatic phylogeny constructed to show organisms from this study compared to other key sequences. (A) Phylogenetic tree of the *Thermus-Deinococcus* group with sequences from this study represented by Glenwood Springs speleothem tip (GSST), speleothem base (GSSB), ceiling mat (GSCM), and cave raft (GSCR). (B) Phylogenetic tree of the green non-sulfur/*Chloroflexus* phyla of *Bacteria*. (C) Phylogenetic tree of the *Crenarchaeota* as they relate to this study.

tained from subsurface depths (>3 km) within deep South African gold mines (47). The next closest relatives to the cave crenarchaeal sequences are various marine “group 1a” *Crenarchaeota*, some of which are capable of ammonia oxidation (27).

The energy sources for organisms in this environment are obscure. To evaluate the possibility that these speleothem-associated crenarchaeotes might have the genetic capacity for ammonia oxidation (AOA), we screened the community DNA from all three samples for putative crenarchaeal ammonia monooxygenase subunit A (*amoA*) genes. These *amoA* genes

have recently been identified in metagenomic libraries (24, 48, 49), in the cultured ammonia-oxidizing archaeon *Nitrosopumilus maritimus* (27), in the sponge symbiont *Cenarchaeum symbiosum* (24), and in a variety of soil (30), water column (14, 21, 28, 35, 52), and sedimentary (21) environments, including an Austrian subsurface radioactive thermal spring with water temperatures of 42°C (51).

Although archaeal 16S rRNA sequences were found in all three stalactite samples, archaeal *amoA* genes were successfully amplified only from the stalactite tip. Phylogenetic analysis of 82 *amoA* sequences from the stalactite tip revealed one

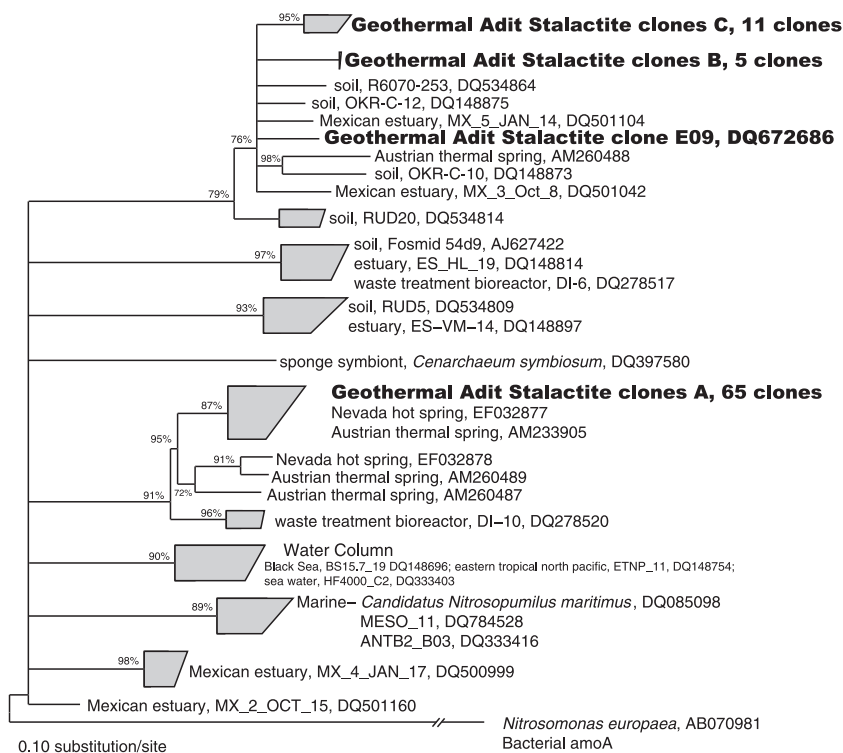


FIG. 5. Diagrammatic phylogenetic tree of the crenarchaeal *amoA* gene diversity associated with the tip of the geothermal speleothem, based on RAXML analysis of nucleotide sequences. Representative database sequences from all known environments where *amoA* has been reported were included in the analysis. Bootstrap values ($>70\%$) are indicated at branch points.

distinct and dominant sequence type (65 of 82 clones with $>98\%$ nucleotide identity; clone group A, a geothermal AOA cluster, in Fig. 5), which is closely related to 3 of 4 sequences reported from the Austrian subsurface thermal spring (51) as well as database sequences from Nevada hot springs (Q. Ye, H. Jiang, H. Dong, and C. Zhang, unpublished data). Two other closely related groups of adit *amoA* sequences, of 5 (group B) and 11 (group C) sequences, respectively, fall into a cluster comprised primarily of sequences from soils and estuarine sediments and of a single Austrian thermal spring sequence. Archaeal *amoA* richness, using 5% and 15% OTU cutoffs at the DNA level, showed only seven and three OTUs, respectively, associated with the stalactite (Chao1-estimated richness analysis in DOTUR [43]). The AOA richness in this unusual environment is fairly low relative to that seen in most other environments analyzed to date (21). However, the temperature at which these organisms are found (50°C), coupled with the similarity of the cave *amoA* gene sequences to those from a subsurface thermal spring (51) and Nevada hot springs, show that crenarchaeota putatively capable of ammonia oxidation are not limited to low-temperature environments. The similarity of gene sequences from these geographically disparate geothermal environments (Colorado, Austria, and Nevada) is also consistent with the notion that geochemically and physically similar environments select for functionally, and in some cases phylogenetically, similar kinds of organisms (45).

DISCUSSION

Microscopic analyses. The $\sim 2\text{-cm}$ soda straw stalactite (Fig. 1A) descends from a dark-colored, microbial biofilm that covers the cave ceiling. The stalactites are hollow (Fig. 1A) and appear to grow downward from the ceiling by a combination of microbial growth and mineral precipitation that forms a fine biofabric around the edge of a water droplet at the tip. We surmise that the soda straw-like speleothems originate as an extension of the microbial community that makes up the biofilm on the adit walls. We postulate that water drops on the ceiling-associated microbial mat initially propagate the mat. It is possible that cellular metabolites and gas exchange alter chemical solubilities in the water and cause mineral precipitation at the air-water interface. With time, microbial cells would become intertwined with these growing crystals, and they indeed may be responsible for their propagation; thus, a cell-mineral-based biofabric thickens into visible layers (Fig. 1B and C). With this process, the community composition shifts in terms of ecological evenness, likely due to changing environmental conditions along the length of the stalactite. Throughout this development, water continues to flow through the center of the cellular and mineral layer outside and the process continues. Eventually, structures of multiple centimeters in length are formed.

Biofabrics and biomineralization. One phenomenon in the stalactite is the intertwining of the mineral matrix and layers of cells (Fig. 1). This might occur as a result of chemical precip-

itation of dissolved compounds in waters or of active biomineralization processes that result from microbial activities. ESEM-EDS shows a disproportionate amount of gypsum and/or sulfate present on and around the cellular forms within the stalactite compared to what is seen for the ceiling biofilm. A second phenomenon is that separate processes seem to occur between the stalactite (with sulfur granules) and the ceiling biofilm (with iron, silica, and oxygen dominant [see Fig. S1 in the supplemental material]). ESEM-EDS shows the presence of both iron oxides and clays between cells, and these minerals accumulate between the biofilm and the hard limestone wall in particular (see Fig. S1 in the supplemental material). The chemical composition of the clays indicates they likely result from acidic dissolution of the limestone matrix due to microbial activities; organic acids of metabolic origin chemically weather the limestone basement rock. Surprisingly, altered rock underneath the biofilm is enriched in both calcium sulfate (gypsum) and calcium phosphate (see Fig. S1 in the supplemental material). Secondary gypsum mineralization processes in karst zones are well documented; however, in the Leadville limestone of central Colorado, calcium phosphates are uncommon (23).

Phylogenetic analyses. The phylogenetic results provide some insight into the processes that likely underlie this ecosystem. If the relative abundances of particular physiological types are taken to reflect the relative amounts of different energy sources that are drawn on for primary productivity, then a census of the microbial community would correspond to the energy demands of the particular environmental niche. The census conducted here yields information about what kinds of cells are present, and from relationships to cultivated relatives, potential metabolic themes for this ecosystem can be proposed (45). For instance, the finding of rRNA genes representative of both *Thermus* spp. and *Hydrogenophilus* spp., whose cultivated relatives oxidize molecular hydrogen (H_2), indicates that H_2 may be a significant electron donor in this subaerial ecosystem. However, most of the organisms detected by sequence are not sufficiently closely related to cultivars with known properties to merit speculation on metabolic lifestyle.

Potential AOA. The identification of putative crenarchaeal *amoA* gene sequences from the speleothem tip indicates that ammonia may serve as an electron donor in this microenvironment. We acknowledge, however, that the detection of these putative *amoA* genes (by PCR) does not confirm activity. The pronounced increase in the abundance of crenarchaeal 16S rRNA gene sequences along the axis of the stalactite suggests that their distribution is controlled by geochemical gradients (Fig. 3). We speculate that ammonia from surface organic matter above could reach the tip of the speleothem as gaseous aerosols in this closed, humid environment. The detection of putative AOA in this unusual low-oxygen environment is consistent with their previous detection in suboxic water columns (e.g., the Black Sea) (14, 21, 28), activated sludge (37), and soil and sediments (21). This study continues to expand not only the range of habitats where AOA occur but also their temperature range up to 50°C.

Although it is not possible to link definitively the crenarchaeal 16S rRNA gene and *amoA* sequences obtained without cultivation or metagenomic approaches, the dominant group of *amoA* sequences from the stalactite tip (geothermal AOA

cluster, group A; Fig. 5) possibly corresponds to the sole South African gold mine *Archaea*-8/group 1.1a-like crenarchaeal 16S rRNA phylotype recovered in this study (Fig. 4C). Support for this stems from the fact the dominant *amoA* sequence type (group A) is more closely related to various marine “water column” sequences (marine group 1.1a *Crenarchaeota*) than to soil-derived sequences likely to be affiliated with the group 1.1b or group 1.1c *Crenarchaeota* (not found in our 16S rRNA clone libraries). In contrast, the other 17 *amoA* sequences (groups B and C; Fig. 5) fall into a cluster comprised primarily of closely related soil and a few sediment sequences, as well as a lone Austrian thermal spring clone sequence (51), consistent with the recovery of group 1.1b-like 16S rRNA sequences from that system. In addition, 16S rRNA sequences closely related to various South African gold mine *Archaea*-like or group 1.1b *Crenarchaeota* were recovered in a previous study of Lechuguilla Cave, New Mexico (36), which suggests that crenarchaeal lineages may be common inhabitants of caves. Of note is the fact that the archaeal sequences recovered from both Lechuguilla Cave and the Austrian thermal spring were obtained with archaea-specific primers (21F and 958R). Thus, although only one dominant crenarchaeal 16S rRNA phylotype was detected within our “universal” clone libraries, it is possible that additional sequence types (e.g., group 1.1b) that correspond to these other AOA would be detected using archaea-specific primers or with more clones examined. Nevertheless, the role of the *Crenarchaeota* and other cave microorganisms in subsurface nitrogen cycling, even at high temperatures, will be the subject of future investigations.

Cave dumplings. Phylogenetically, the most complex community in this vapor cave surrounds the dumplings that float on the surface of cave floor pools (Fig. 3). The complexity confounds efforts to interpret a nutritional basis for the dumpling community. Of note, however, is the fact that 14% of the library is composed of relatives (99% rRNA sequence identity) of heterotrophic organisms isolated from other caves. This subspecies relationship suggests that much of the community thrives on organics provided in the hot water. ESEM-EDS indicates that the dumplings have a gypsum core wrapped within a complex biofabric of microbiota (Fig. 2) embedded in what appears to be EPS wrapped around gypsum crystals and between cells. In addition to the thickness of the biofabric around the mineral matrix, this biofabric surface enclosure likely prevents the highly soluble gypsum from dissolving in the 50°C water. Such a hypothesis is supported by the observation that when a dumpling is physically damaged, disrupting the microbial fabric, dissolution of the precipitated gypsum is immediate.

Conclusions. We have found that microbial mats line nearly every surface of this geothermal mine adit and form distinct communities comprised of novel organisms, many only distantly related to known organisms. Thus, the study expands known phylogenetic diversity. We focused on communities that occur as biofabrics, organized in arrays of cellular structures that lend structural strength to the mineralized component. Such fabric-like structures probably are common in mineral-based environments such as soils and sediments and are little studied. Fabric-like structure could play a significant role in the maintenance and propagation of the communities that make up the natural microbial world.

Our results also confirm the known temperature range where putative AOA are likely to be found to 50°C and expand the broad range of habitats where these organisms may persist if not thrive. Finally, we suggest that given the amount and extent of microbial diversity present in the examined speleothems, microbiota may play a more significant role in many speleothem formations than is currently acknowledged.

ACKNOWLEDGMENTS

Support for this work to J.R.S. came from a geobiology postdoctoral fellowship from the Agouron Institute. Support for H.A.B. comes from the Center for Integrated Natural Science and Mathematics at NKU with infrastructure support from the NIH KY-INBRE program. N.R.P. is supported by funds from the NASA Astrobiology Institute.

We thank members of the Colorado caving community who assisted with this project, including Donald Davis, Douglas Medville, Richard Rhinehart, and Fred Luiszer. At NKU, we thank Nicholas Taylor for assistance with rock extraction techniques and Karl Hagglund for assistance with ESEM-EDS imaging. Thanks to Katie Roberts for her early contribution to this project and to members of the Pace and Spear labs and Jason Sahl for assistance and thoughtful reviews of this work.

REFERENCES

- Altschul, S. F., T. L. Madden, A. A. Schäffer, J. Zhang, Z. Zhang, W. Miller, and D. J. Lipman. 1997. Gapped BLAST and PSI-BLAST: a new generation of protein database search programs. *Nucleic Acids Res.* **25**:3389–3402.
- Ashelford, K. E., N. A. Chuzhanova, J. C. Fry, A. J. Jones, and A. J. Weightman. 2006. New screening software shows that most recent large 16S rRNA gene clone libraries contain chimeras. *Appl. Environ. Microbiol.* **72**:5734–5741.
- Auler, A. S., and P. L. Smart. 2001. Late quaternary paleoclimate in semi-arid northeastern Brazil from U-series dating of travertine and water-table speleothems. *Quat. Res.* **55**:159–167.
- Ayliffe, L. K., and H. H. Veeh. 1988. Uranium-series dating of speleothems and bones from Victoria Cave, Naracoorte, South Australia. *Chem. Geol.* **72**:211–234.
- Bar-Matthews, M., A. Avalon, M. Gilmour, A. Matthews, and C. J. Hawkesworth. 2003. Sea-land oxygen isotopic relationships from planktonic foraminifera and speleothems in the eastern Mediterranean region and their implication for paleorainfall during interglacial intervals. *Geochim. Cosmochim. Acta* **67**:3181–3199.
- Barton, H. A. 2006. Introduction to cave geomicrobiology: a review for the nonspecialist. *J. Cave Karst Stud.* **68**:43–54.
- Barton, H. A., J. R. Spear, and N. R. Pace. 2001. Microbial life in the underworld: biogenicity, in secondary mineral formations. *Geomicrobiol. J.* **18**:359–368.
- Barton, H. A., and F. Luiszer. 2005. Microbial metabolic structure in a sulfidic cave hot spring: potential mechanisms of biospeleogenesis. *J. Cave Karst Stud.* **67**:28–38.
- Ben-Ari, E. T. 2002. Microbiology and geology: solid marriage made on Earth. *ASM News* **68**:13–18.
- Bininda-Emonds, O. R. 2005. transAlign: using amino acids to facilitate the multiple alignment of protein-coding DNA sequences. *BMC Bioinformatics* **6**:156.
- Bosak, T., and D. K. Newman. 2005. Microbial kinetic controls on calcite morphology in supersaturated solutions. *J. Sediment. Res.* **75**:190–199.
- Braissant, O., G. Cailleau, C. Dupraz, and E. P. Verrecchia. 2005. Bacterially induced mineralization of CaCO₃ in terrestrial environments: the role of exopolysaccharides and amino acids. *J. Sediment. Res.* **73**:485–490.
- Brigmon, R. L., et al. 1994. Biogeochemical ecology of *Thiothrix* spp. in underwater limestone caves. *Geomicrobiol. J.* **12**:141–159.
- Coolen, M. J., B. Abbas, J. van Bleijswijk, E. C. Hopmans, M. M. Kuypers, S. G. Wakeham, and J. S. Sinninghe Damste. 2007. Putative ammonia-oxidizing Crenarchaeota in suboxic waters of the Black Sea: a basin-wide ecological study using 16S ribosomal and functional genes and membrane lipids. *Environ. Microbiol.* **9**:1001–1016.
- Cunningham, K. I., et al. 1995. Bacteria, fungi, and biokarst in Lechuguilla Cave, Carlsbad Caverns National Park, New Mexico. *Environ. Geol.* **25**:2–8.
- DeSantis, T. Z., P. Hugenholtz, N. Larsen, M. Rojas, E. L. Brodie, K. Keller, T. Huber, D. Dalevi, P. Hu, and G. L. Andersen. 2006. Greengenes, a chimera-checked 16S rRNA gene database and workbench compatible with ARB. *Appl. Environ. Microbiol.* **72**:5069–5072.
- DeSantis, T. Z., Jr., P. Hugenholtz, K. Keller, E. L. Brodie, N. Larsen, Y. M. Piceno, R. Phan, and G. L. Andersen. 2006. NAST: a multiple sequence alignment server for comparative analysis of 16S rRNA genes. *Nucleic Acids Res.* **34**:W394–W399.
- Dojka, M. A., P. Hugenholtz, S. K. Haack, and N. R. Pace. 1998. Microbial diversity in a hydrocarbon- and chlorinated-solvent-contaminated aquifer undergoing intrinsic bioremediation. *Appl. Environ. Microbiol.* **64**:3869–3877.
- Engel, A. S., N. Lee, M. L. Porter, L. A. Stern, P. C. Bennett, and M. Wagner. 2003. Filamentous “*Epsilonproteobacteria*” dominate microbial mats from sulfidic cave springs. *Appl. Environ. Microbiol.* **69**:5503–5511.
- Engel, A. S., M. L. Porter, L. A. Stern, S. Quinlan, and P. C. Bennett. 2004. Bacterial diversity and ecosystem function of filamentous microbial mats from aphotic (cave) sulfidic springs dominated by chemolithoautotrophic *Epsilonproteobacteria*. *FEMS Microbiol. Ecol.* **51**:31–53.
- Francis, C. A., K. J. Roberts, J. M. Beman, A. E. Santoro, and B. B. Oakley. 2005. Ubiquity and diversity of ammonia-oxidizing archaea in water columns and sediments of the ocean. *Proc. Natl. Acad. Sci. USA* **102**:14683–14688.
- Frankel, R. B., and D. A. Bazylinski. 2003. Biologically induced mineralization by bacteria. *Rev. Mineral. Geochem.* **54**:95–114.
- Geldon, A. L. 1989. Hydrogeology of the Leadville limestone and other paleozoic rocks in northwestern Colorado, with results of aquifer tests at Glenwood Springs. U.S. Geological Survey, Denver, CO.
- Hallam, S. J., T. J. Mincer, C. Schleper, C. M. Preston, K. Roberts, P. M. Richardson, and E. F. DeLong. 2006. Pathways of carbon assimilation and ammonia oxidation suggested by environmental genomic analyses of marine Crenarchaeota. *PLoS Biol.* **4**:e95.
- Huber, T., G. Faulkner, and P. Hugenholtz. 2004. Bellerophon: a program to detect chimeric sequences in multiple sequence alignments. *Bioinformatics* **20**:2317–2319.
- Klimchouk, A. B., D. C. Ford, A. N. Palmer, and W. Dreybrodt. 2000. Speleogenesis: evolution of karstic aquifers. National Speleological Society, Huntsville, AL.
- Konneke, M., A. E. Bernhard, J. R. de la Torre, C. B. Walker, J. B. Waterbury, and D. A. Stahl. 2005. Isolation of an autotrophic ammonia-oxidizing marine archaeon. *Nature* **437**:543–546.
- Lam, P., M. M. Jensen, G. Lavik, D. F. McGinnis, B. Muller, C. J. Schubert, R. Amann, B. Thamdrup, and M. M. Kuypers. 2007. Linking crenarchaeal and bacterial nitrification to anammox in the Black Sea. *Proc. Natl. Acad. Sci. USA* **104**:7104–7109.
- Lane, D. J. 1991. 16S/23S rRNA sequencing, p. 115–175. *In* E. Stackebrandt and M. Goodfellow (ed.), *Nucleic acid techniques in bacterial systematics*. John Wiley and Sons, New York, NY.
- Leininger, S., T. Urich, M. Schloter, L. Schwark, J. Qi, G. W. Nicol, J. I. Prosser, S. C. Schuster, and C. Schleper. 2006. Archaea predominate among ammonia-oxidizing prokaryotes in soils. *Nature* **442**:806–809.
- Lozupone, C., and R. Knight. 2005. UniFrac: a new phylogenetic method for comparing microbial communities. *Appl. Environ. Microbiol.* **71**:8228–8235.
- Ludwig, W., O. Strunk, R. Westram, L. Richter, H. Meier, Yadhukumar, A. Buchner, T. Lai, S. Steppi, G. Jobb, W. Forster, I. Brettske, S. Gerber, A. W. Ginhart, O. Gross, S. Grumann, S. Hermann, R. Jost, A. König, T. Liss, R. Lussmann, M. May, B. Nonhoff, B. Reichel, R. Strehlow, A. Stamatakis, N. Stuckmann, A. Vilbig, M. Lenke, T. Ludwig, A. Bode, and K. H. Schleifer. 2004. ARB: a software environment for sequence data. *Nucleic Acids Res.* **32**:1363–1371.
- Mattison, R. G., M. Abbiati, P. R. Dando, M. F. Fitzsimons, S. M. Pratt, A. J. Southward, and E. C. Southward. 1998. Chemoautotrophic microbial mats in submarine caves with hydrothermal sulphidic springs at Cape Palinuro, Italy. *Microb. Ecol.* **35**:58–71.
- Melim, L. A., K. M. Shingman, P. J. Boston, D. E. Northup, M. N. Spilde, and J. M. Queen. 2001. Evidence for microbial involvement in pool finger precipitation, Hidden Cave, New Mexico. *Geomicrobiol. J.* **18**:311–329.
- Mincer, T. J., M. J. Church, L. T. Taylor, C. M. Preston, D. M. Karl, and E. F. DeLong. 2007. Quantitative distribution of presumptive archaeal and bacterial nitrifiers in Monterey Bay and the North Pacific Subtropical Gyre. *Environ. Microbiol.* **9**:1162–1175.
- Northup, D. E., S. M. Barns, L. E. Yu, M. N. Spilde, R. T. Schelble, K. E. Dano, L. J. Crossey, C. A. Connolly, P. J. Boston, D. O. Natvig, and C. N. Dahm. 2003. Diverse microbial communities inhabiting ferromanganese deposits in Lechuguilla and Spider Caves. *Environ. Microbiol.* **5**:1071–1086.
- Park, H. D., G. F. Wells, H. Bae, C. S. Criddle, and C. A. Francis. 2006. Occurrence of ammonia-oxidizing archaea in wastewater treatment plant bioreactors. *Appl. Environ. Microbiol.* **72**:5643–5647.
- Sarbu, S. M., T. C. Kane, and B. K. Kinkle. 1996. A chemoautotrophically based cave ecosystem. *Science* **272**:1953–1955.
- Schabereiter-Gurtner, C., et al. 2003. Phylogenetic diversity of bacteria associated with Paleolithic paintings and surrounding rock walls in two Spanish caves (Llonin and La Garma). *FEMS Microbiol. Ecol.* **47**:235–247.
- Schabereiter-Gurtner, C., G. Pinar, D. Vybiral, W. Lubitz, and S. Rolfeke. 2001. *Rubrobacter*-related bacteria associated with rosy discoloration of masonry and lime wall paintings. *Arch. Microbiol.* **176**:347–354.
- Schabereiter-Gurtner, C., C. Saiz-Jimenez, G. Pinar, W. Lubitz, and S. Rolfeke. 2002. Altamira cave Paleolithic paintings harbor partly unknown bacterial communities. *FEMS Microbiol. Lett.* **211**:7–11.
- Schabereiter-Gurtner, C., C. Saiz-Jimenez, G. Pinar, W. Lubitz, and S. Rolfeke. 2002. Phylogenetic 16S rRNA analysis reveals the presence of com-

- plex and partly unknown bacterial communities in Tito Bustillo cave, Spain, and on its Paleolithic paintings. *Environ. Microbiol.* **4**:392–400.
43. **Schloss, P. D., and J. Handelsman.** 2005. Introducing DOTUR, a computer program for defining operational taxonomic units and estimating species richness. *Appl. Environ. Microbiol.* **71**:1501–1506.
 44. **Simkiss, K., and K. M. Wilbur.** 1989. *Biomineralization: cell biology and mineral deposition.* Academic Press, San Diego, CA.
 45. **Spear, J. R., J. J. Walker, T. M. McCollom, and N. R. Pace.** 2005. Hydrogen and bioenergetics in the Yellowstone geothermal ecosystem. *Proc. Natl. Acad. Sci. USA* **102**:2555–2560.
 46. **Stamatakis, A.** 2006. RAxML-VI-HPC: maximum likelihood-based phylogenetic analyses with thousands of taxa and mixed models. *Bioinformatics* **22**:2688–2690.
 47. **Takai, K., D. P. Moser, M. DeFlaun, T. C. Onstott, and J. K. Fredrickson.** 2001. Archaeal diversity in waters from deep South African gold mines. *Appl. Environ. Microbiol.* **67**:5750–5760.
 48. **Treusch, A. H., S. Leininger, A. Kletzin, S. C. Schuster, H. P. Klenk, and C. Schleper.** 2005. Novel genes for nitrite reductase and Amo-related proteins indicate a role of uncultivated mesophilic crenarchaeota in nitrogen cycling. *Environ. Microbiol.* **7**:1985–1995.
 49. **Venter, J. C., K. Remington, J. F. Heidelberg, A. L. Halpern, D. Rusch, J. A. Eisen, D. Wu, I. Paulsen, K. E. Nelson, W. Nelson, D. E. Fouts, S. Levy, A. H. Knap, M. W. Lomas, K. Nealson, O. White, J. Peterson, J. Hoffman, R. Parsons, H. Baden-Tillson, C. Pfannkoch, Y. H. Rogers, and H. O. Smith.** 2004. Environmental genome shotgun sequencing of the Sargasso Sea. *Science* **304**:66–74.
 50. **Walker, J. J., J. R. Spear, and N. R. Pace.** 2005. Geobiology of a microbial endolithic community in the Yellowstone geothermal environment. *Nature* **434**:1011–1014.
 51. **Weidler, G. W., M. Dornmayr-Pfaffenhuemer, F. W. Gerbl, W. Heinen, and H. Stan-Lotter.** 2007. Communities of *Archaea* and *Bacteria* in a subsurface radioactive thermal spring in the Austrian Central Alps, and evidence of ammonia-oxidizing *Crenarchaeota*. *Appl. Environ. Microbiol.* **73**:259–270.
 52. **Wuchter, C., B. Abbas, M. J. Coolen, L. Herfort, J. van Bleijswijk, P. Timmers, M. Strous, E. Teira, G. J. Herndl, J. J. Middelburg, S. Schouten, and J. S. Sinninghe Damste.** 2006. Archaeal nitrification in the ocean. *Proc. Natl. Acad. Sci. USA* **103**:12317–12322.